

Low-cost optical fiber temperature-sensing system employing optical transceivers for Ethernet and long-period fiber grating

著者	Koyama Osanori, Matsui Makoto, Kagawa Takuro, Suzuki Yuta, Ikeda Kanami, Yamada Makoto
journal or publication title	Applied Optics
volume	58
number	9
page range	2366-2371
year	2019-03-19
権利	(C) 2019 Optical Society of America. Users may use, reuse, and build upon the article, or use the article for text or data mining, so long as such uses are for non-commercial purposes and appropriate attribution is maintained. All other rights are reserved.
URL	http://hdl.handle.net/10466/00017171

doi: <https://doi.org/10.1364/AO.58.002366>

Low-cost optical fiber temperature-sensing system employing optical transceivers for Ethernet and long-period fiber grating

OSANORI KOYAMA,^{1,*} MAKOTO MATSUI,¹ TAKURO KAGAWA,¹ YUTA SUZUKI,¹
KANAMI IKEDA,¹ MAKOTO YAMADA¹

¹Department of Elec. and Info. Systems, Osaka Prefecture University, 1-1 Gakuen-cho, Nakaku, Sakai, Osaka 599-8531, Japan

*Corresponding author: koyama@eis.osakafu-u.ac.jp

Received XX Month XXXX; revised XX Month, XXXX; accepted XX Month XXXX; posted XX Month XXXX (Doc. ID XXXXX); published XX Month XXXX

Optical fiber sensors have numerous advantages over electrical sensors. However, in some cases, sensing systems based on optical fiber sensors are inferior to electrical sensors in terms of cost because expensive instruments are required. Therefore, cost-effective options must be developed. Herein, inexpensive optical transceivers (OTRs) for Ethernet were used instead of a broadband light source and optical spectrum analyzer; a CO₂ laser-induced long-period fiber grating (LPFG) was used as a temperature sensor. The sensing system was implemented by introducing OTRs and LPFG in an experimental Internet protocol (IP) over Ethernet. The results showed that a low-cost sensing system can estimate the ambient temperature of the LPFG based on the no-reply rate for the internet control message protocol echo request. As regards the sensing performance, the measurable range was ~100°C with ±4.5°C errors. © 2018 Optical Society of America

<http://dx.doi.org/10.1364/AO.99.099999>

1. INTRODUCTION

Long-period fiber grating (LPFG) are a type of in-fiber refractive-index grating, wherein light from the fundamental core propagation mode is coupled to forward propagating cladding modes. The LPFG causes high attenuation of the input light at a specified wavelength, known as the resonant wavelength [1], based on the LPFG coupling characteristics. The resonant wavelength is dependent on the temperature, showing a linear relation with the temperature near the LPFG. Therefore, the temperature can be estimated by monitoring the resonant wavelength of an LPFG installed at the target measurement location. Several studies on temperature sensing using an LPFG have been reported earlier [2–6].

Optical fiber sensors consisting of an LPFG have many advantages over conventional electrical sensors: noninterference with electromagnetic waves, the ability to activate the sensor unit without a power source, and remote monitoring capability over several kilometers without repeaters. However, in some cases, optical fiber sensing systems are inferior to electrical sensing systems in terms of cost, because expensive instruments are used in optical fiber sensing systems, such as a broadband light source to input light into the optical fiber sensor, optical spectrum analyzer (OSA), and optical power meter to analyze transmitted light. Therefore, cost-effective options should be developed to enhance the practicality of optical fiber sensor systems. Even though the measurable range and accuracy of the options are

narrower and less than them of conventional optical fiber sensing systems, the options can be used for relatively rough monitoring with a low introducing cost. Some studies have reported on low-cost optical fiber sensing systems in which photodetectors were used instead of optical power meters [7]. Also, an 850-nm inexpensive light source was used [8, 9].

We proposed a low-cost optical fiber temperature-sensing system in which a pair of inexpensive optical transceivers (OTRs), used for optical internet protocol (IP) networks, and Ethernet are employed instead of a broadband light source and OSA; an LPFG fabricated by a CO₂ laser is used as an optical fiber temperature sensor [10]. The inexpensive OTRs are several hundred dollars, and are much cheaper than mid-level OSA and broadband light source. Moreover, a suitable condition for the loss spectrum of the LPFG has been defined for the proposed system, and the LPFG fabrication results that satisfy this condition have been reported in Ref. [10]. Herein, we demonstrate that our system can conduct temperature sensing using the previously reported pair of inexpensive OTRs and the suitable LPFG in an experimental optical IP over Ethernet. The experimental results are discussed subsequently.

2. Temperature-sensing system employing OTRs and LPFG in IP over Ethernet

Figure 1 presents a schematic of the proposed temperature-sensing system. The system consists of an LPFG as a temperature sensor, a pair

of layer-3 switches (L3SWs) for transmitting IP packets, a single-mode optical fiber (SMF) for connecting the LPFG and the L3SWs, a pair of OTRs for converting electrical signals to optical signals, a variable optical attenuator (VOA), and a computer for estimating the temperature. The LPFG is fabricated by CO₂ laser irradiation and also satisfies the conditions that are described in Section 3. It is assumed that the system employs unused ports in the existing L3SWs, which are still installed at the user's location; for example, in a business building, school, hospital, or a large-scale plant. Therefore, the cost of the newly purchased L3SWs is not included in the total cost of the system. The fiber is a commercially available SMF (SMF-28). The OTRs are inexpensive and compatible with numerous Ethernet switches, such as gigabit interface converters (GBIC), small form-factor pluggable (SFP) transceivers, and 10-gigabit SFP (XFP) transceivers. The VOA is used to adjust the optical power received at the receiving-side OTR. The computer, which is similar to a personal computer (PC), sends an internet control message protocol (ICMP) Echo request and receives an ICMP Echo reply [11]. When the receiving-side L3SW (as shown in right L3SW in Fig. 1) receives an ICMP Echo request packet in the normal manner, it sends back an ICMP Echo reply packet. Most computers can exchange ICMP packets with other network instruments. The PC calculates the ICMP Echo no-reply rate depending on the temperature and estimates the temperature near the LPFG.

Figure 2 shows the temperature-sensing mechanism employed in this system. In the top left region of Fig. 2, the power spectrum of the light output from the sending-side OTR and the loss spectrum of the LPFG in the default state are shown. The wavelength for which the output light has the highest power and the attenuation wavelength band of the LPFG are adjusted to prevent any overlap. In this way, the received power at the receiving-side OTR exceeds the minimum allowable power of the OTR, although the light passing through the LPFG experiences a slight optical loss. Therefore, the receiving-side OTR can normally receive all of the ICMP Echo request packets from the measurement PC in the default state, as shown in the top right region of Fig. 2. Then, the ICMP Echo reply packets can be sent back to the measurement PC. As a result, the ICMP Echo no-reply rate becomes 0%. When the ambient temperature of the LPFG increases from the default value, the attenuation band of the LPFG shifts to a longer wavelength, as shown in the lower left region of Fig. 2. As the temperature increases, the overlap between the power spectrum and the loss spectrum increases. The output light is gradually attenuated by the LPFG, and consequently, the received power decreases. Thus, the received power can be correlated with the ambient temperature of the LPFG.

If the system measures the received power at the receiving-side OTR, the system can estimate the temperature based on the correlation. However, storage about the received power is not implemented in the management information base (MIB) [12] of typical L3SWs. The received power cannot be obtained by investigating the MIB with a simple network management protocol (SNMP) [13]. Therefore, the change in received power must be associated with one of the IP network characteristics.

Generally, the minimum allowable light power of the OTR has a range R (as shown in the upper right region of Fig. 2), wherein an IP packet can be received with a probability depending on the power received at the receiving-side OTR. If the received power is less than the lower limit of R , the ICMP Echo request packet generally cannot be received by the OTR; as a result, the ICMP Echo no-reply rate is 100%, indicating that there are no ICMP Echo reply packets corresponding to the ICMP Echo request packets from the sending-side OTR. Conversely, when the received power is higher than the upper limit of R , the no-reply rate becomes 0%, indicating that all ICMP Echo request packets have a corresponding ICMP Echo reply packet. When the received power is in the range R , the no-reply rate increases as the received power decreases.

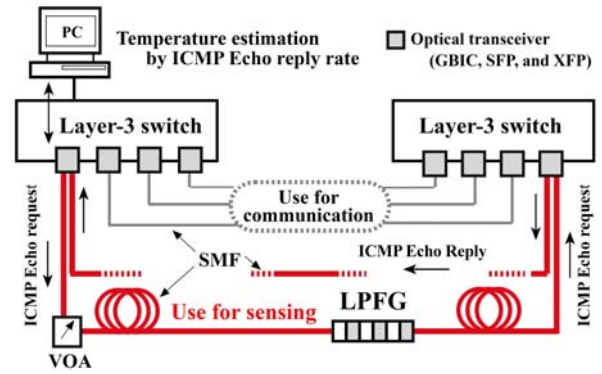


Fig. 1. Temperature-sensing system employing OTRs and an LPFG.

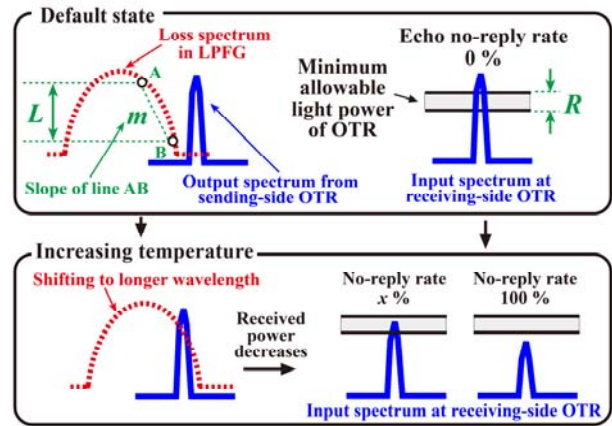


Fig. 2. Mechanism of temperature sensing.

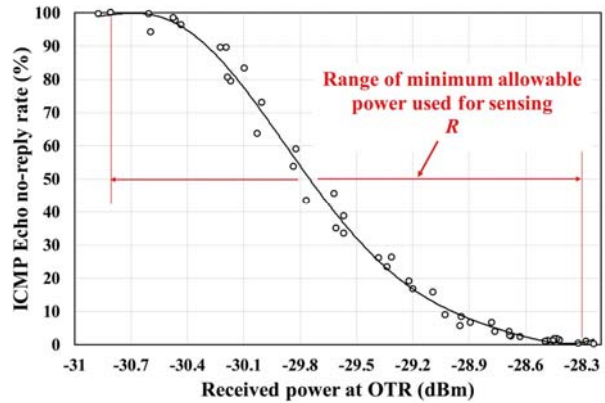


Fig. 3. Relation between the received power and the ICMP Echo no-reply rate.

The OTRs used in this study exhibit a characteristic relation between the received power and the ICMP Echo no-reply rate, as shown in Fig. 3 [14]. The range R of the OTRs is also shown in Fig. 3. To initialize the system to the default state shown in Fig. 2, the power received at the receiving-side OTR is adjusted to the upper limit in the range R using the VOA.

With this initialization, the received power can be correlated to the no-reply rate; thus, the ambient temperature of the LPFG can be estimated from the no-reply rate.

3. LPFG fabrication

We define the lower and upper limits of the temperature range in the system as T_1 and T_2 , respectively. The minimum allowable light power range of the OTR in the system is defined as R (shown in Figs. 2 and 3), and the linear temperature coefficient of the LPFG is defined as α , which specifies the linear relationship between the shifting of the LPFG's loss spectrum to longer wavelength and the increase in temperature near the LPFG.

Next, two conditions on the LPFG's loss spectrum for this system are defined as below. Assuming that the slope of the LPFG loss spectrum in the region used for temperature sensing is m (as shown in Fig. 2), one of the conditions can be expressed as (1)

$$m \leq \frac{R}{\alpha(T_2 - T_1)}. \quad (1)$$

The unit of m is dB/nm.

Furthermore, assuming that the attenuation range of the loss spectrum is L (as shown in Fig. 2), the second condition is expressed as (2)

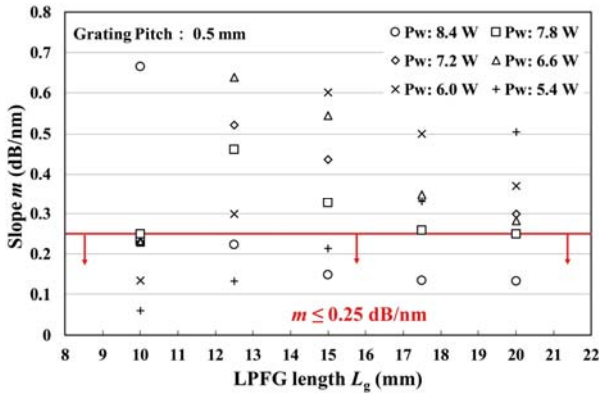


Fig. 4. Slope of the attenuation band in the loss spectra of the fabricated LPFGs.

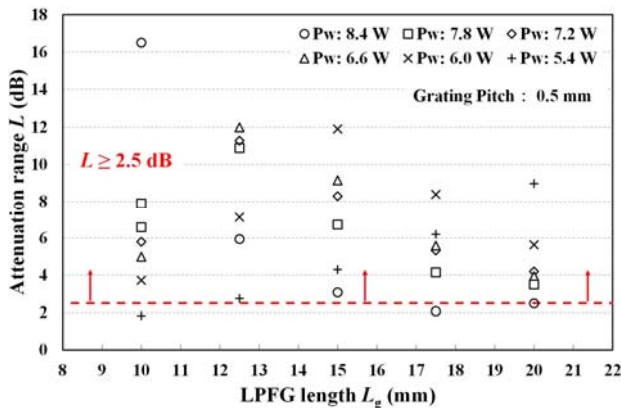


Fig. 5. Attenuation ranges of the attenuation band in the loss spectra of the fabricated LPFGs.

$$L \geq R. \quad (2)$$

The unit of L is dB.

Herein, we assume a suitable loss spectrum for the system to simultaneously satisfy Eqs. (1) and (2). The above-mentioned parameters were set as follows: $T_2 - T_1 = 100^\circ\text{C}$, $R = 2.5$ dB, and $\alpha = 0.1$ nm/ $^\circ\text{C}$. The value $R = 2.5$ dB is employed because the minimum allowable power of the OTRs used was 2.5 dB, and $\alpha = 0.1$ nm/ $^\circ\text{C}$ is utilized because the average linear temperature coefficient of the LPFG fabricated in our laboratory was 0.1 nm/ $^\circ\text{C}$. Therefore, two conditions were obtained as following equations:

$$m \geq 0.25, \quad (3)$$

$$L \geq 2.5. \quad (4)$$

To fabricate the LPFGs, a CO₂ laser was used [15]. The grating pitch of each LPFG was set to 0.5 mm, and 31 LPFG samples were fabricated by varying the LPFG length L_g from 10 mm to 20 mm, and the irradiation power P_w of the CO₂ laser from 5.4 W to 8.4 W. Figure 4 shows the slopes m for the loss spectrum of the fabricated LPFGs. All values of m and L were obtained over a range from 20% larger than the bottom of the attenuation band in the loss spectrum to 20% smaller than the attenuation peak (as shown in Fig. 2). The number of LPFGs satisfying the first condition was 14, as shown in Fig. 4, and the number of LPFGs satisfying the second condition was 28, as shown in Fig. 5. Thus, we successfully fabricated 10 LPFGs that simultaneously satisfied the two conditions. Table 1 summarizes the fabrication parameters and evaluation items for the LPFGs.

Table 1. Fabrication parameters for LPFGs satisfying two conditions

#	P_w (W)	L_g (mm)	Evaluation Items (measured at room temperature)	
			m (dB/nm)	L (dB)
1	5.4	12.5	0.13	2.7
2	5.4	15.0	0.21	4.3
3	6.0	10.0	0.13	3.7
4	6.6	10.0	0.23	5.0
5	7.2	10.0	0.23	5.8
6	7.8	10.0	0.23	6.6
7	7.8	10.0	0.25	7.9
8	7.8	20.0	0.25	3.5
9	8.4	12.5	0.22	5.9
10	8.4	15.0	0.15	3.1

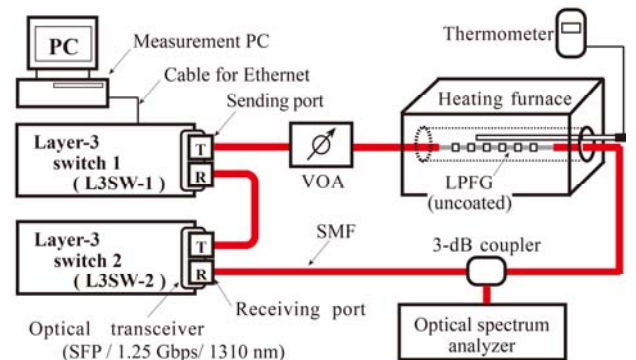


Fig. 6. Experimental setup.

4. Experiment and discussion

We assessed whether the system could perform temperature sensing by using a pair of OTRs and the fabricated LPFG. Figure 6 shows the experimental setup. Each OTR (SCPEN4-GL-ZN-31, Sumitomo Electric) is in the SFP format with a data transmission speed of 1.25 Gbps and an output wavelength of 1310 nm. We prepared two L3SWs (CentreCOM 8948XL, Allied Telesis) for IP routing, and each L3SW was equipped with an OTR, as mentioned above. The sending port of the OTR in L3SW-1 and a VOA were connected by an SMF, and an uncoated LPFG located in a heating furnace was connected to the VOA. Sample 7, described in Table 1, was used as the LPFG. The receiving port of the OTR in L3SW-2 was connected to the end of the LPFG. To measure the optical power at the receiving port of the OTR, an OSA was installed in the experimental setup with a 3-dB coupler. The sending port of the OTR in L3SW-2 and the receiving port of the OTR in L3SW-1 had to be connected to send ICMP Echo reply packets back to the measurement PC. The measurement PC sent ICMP Echo request packets to L3SW-2. When L3SW-2 could receive the packets in a normal manner, ICMP Echo reply packets were sent back to the measurement PC. However, when the received light power falls below the minimum allowable light power of the OTR, L3SW-2 could not receive the packets normally and could not send reply packets back to the measurement PC. The temperature inside the heating furnace was measured using a thermocouple temperature sensor.

In this experiment, the target temperature was set from 90°C (T_1) to 190°C (T_2). As the initial setting, when the temperature inside the heating furnace was 90°C, the light power received at the receiving-side OTR in L3SW-2 was adjusted to -28.5 dBm using the VOA. Thereafter, the temperature in the heating furnace was increased to 200°C at a rate of approximately 0.8°C/min. Figure 7 shows the temperature dependence of the optical loss spectrum shift for the LPFG used in this experiment. As the temperature increased, the entire spectrum shifted to longer wavelengths. Figure 8 shows the light spectrum received at the receiving-side OTR in L3SW-2 for furnace temperatures of 91.6°C and 200.3°C. Figure 8 shows that the light power received at 1310 nm decreased approximately 2.6 dB. This decrease occurred because the loss value at 1310 nm in the optical loss spectrum, as shown in Fig. 7, increased by approximately 2.3 dB as the temperature increased inside the heating furnace. It is inferred that the difference of 0.3 dB was caused by the difference between the furnace temperatures of 189.4°C in Fig. 7 and 200.3°C in Fig. 8. As the temperature in the heating furnace increased, ICMP Echo request packets were sent from the measurement PC and received by L3SW-2. The ICMP Echo no-reply rate was calculated as a function of temperature by the measurement PC. The ICMP Echo no-reply rate was derived from the total number of ICMP Echo request packets sent by the measurement PC and the total number of ICMP Echo reply packets received by the measurement PC. Here, the number of request packets was set to 200 for each temperature. For each temperature, the calculation was repeated 5 times, and the average value was obtained. The measurement results and an approximate curve are shown in Fig. 9. The measurement PC estimated the temperature near the LPFG using the approximate curve based on the calculated ICMP no-reply rate.

The temperature error range based on the approximate curve was approximately $\pm 4.5^\circ\text{C}$. It is expected that the temperature error was related to R that was only ~ 2.5 dB and was also related to the nonlinearity of the relationship between ICMP Echo no-reply rate and the received power at OTR. The temperature error is larger than conventional temperature sensing systems with LPFG. However, the proposed system can monitor the temperature roughly by adding it to the existing IP over Ethernet set-up with low additional cost. For example, it is expected that the proposed system can be used for high-

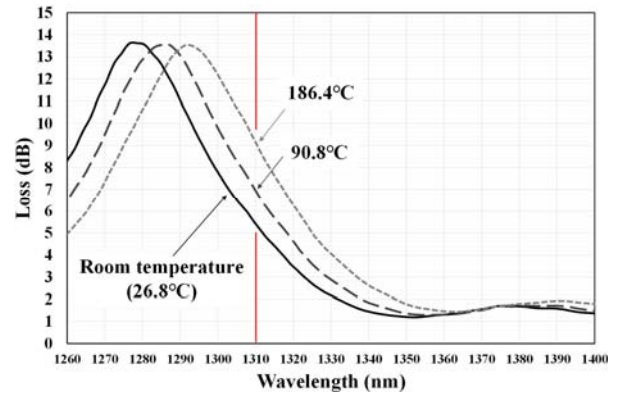


Fig. 7. Temperature dependence of the shift in the LPFG optical loss spectrum.

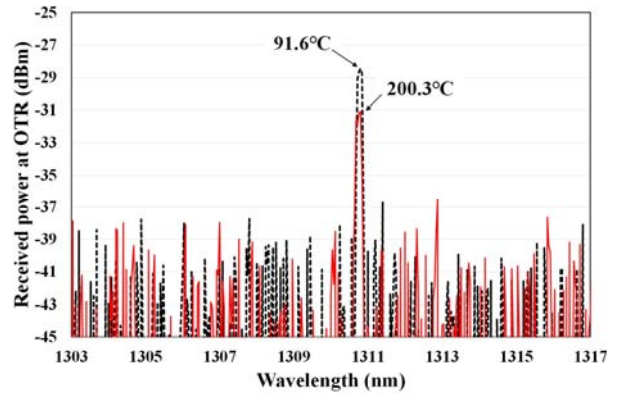


Fig. 8. Light spectrum received at the receiving-side OTR.

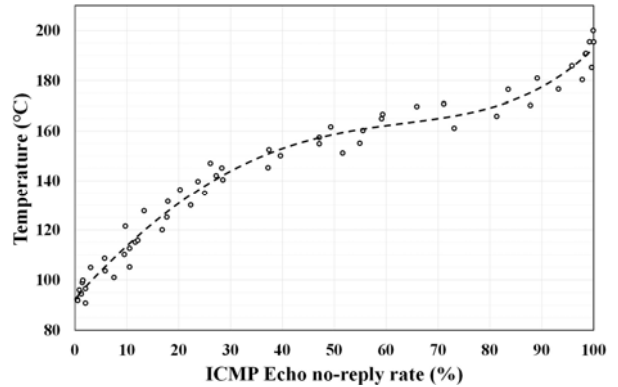


Fig. 9. Relation between ICMP Echo no-reply rate and the furnace temperature.

temperature alarming by detecting that ICMP Echo no-reply rate exceeds a certain threshold value.

From the viewpoint of improving the function of the temperature-sensing system, it is expected that the measurable temperature range can be expanded by making R larger, m smaller and α smaller, because the range depends on R , m and α as described in equation (1). As regards making m smaller, it is expected that the measurable temperature range becomes $\sim 192^\circ\text{C}$, if sample 1 described in Table 1 is used. With further additional cost, it is expected that the measurable temperature range

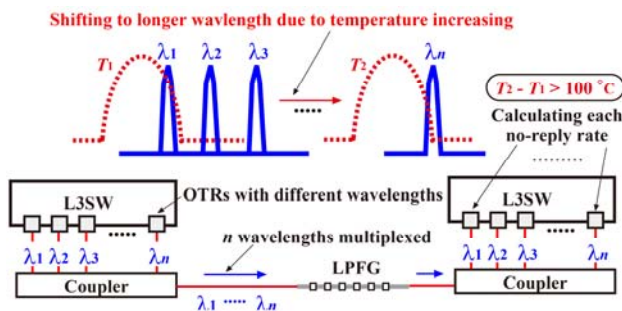


Fig. 10. Measurable temperature range expanded by n OTRs.

can be expanded largely using OTRs with different output wavelengths and by installing two couplers to multiplex and demultiplex the wavelengths, as shown in Fig. 10. By calculating the ICMP Echo no-reply rate with each OTR, it is expected that a range of more than 100°C can be sensing. Also, it is expected that temperatures up to approximately 800°C can be measured because CO₂ laser-induced LPFGs can maintain the relationship between increasing temperature and resonant wavelength shifting at high temperatures as reported in Ref. [2-6] compared with fiber gratings fabricated by ultraviolet laser irradiation [16].

Thus, we successfully performed temperature sensing based on the ICMP Echo no-reply rate using an LPFG and inexpensive OTRs installed in an IP over Ethernet.

5. Conclusion

To realize a low-cost temperature-sensing system in an IP over Ethernet, we employed two inexpensive OTRs as a light source and a receiver, a CO₂ laser-induced LPFG, two L3SWs, and a measurement PC. The temperature was estimated from the ICMP Echo no-reply rate calculated by the measurement PC. We demonstrated that this temperature-sensing method can be applied in an experimental network. A temperature range of approximately 100°C could be measured, although there were approximately ±4.5°C errors. In terms of future work, we will clarify the LPFG fabrication parameters to fabricate LPFGs suitable for the system, expand the measurable temperature range of the system, and investigate the feasibility of using the system at high temperatures.

Funding Information. Japan Society for the Promotion of Science (JSPS) (16K06306)

Acknowledgment. This work was supported by JSPS KAKENHI Grant Number 16K06306.

References

1. A. M. Vengsarkar, P. J. Lemaire, J. B. Judkins, V. Bhatia, T. Erdogan, and J. E. Sipe, "Long-period fiber gratings as band-rejection filters," *J. Lightwave Technol.* **14**(1), 58-65 (1996).
2. D. D. Davis, T. K. Gaylord, E. N. Glytsis, and S. C. Mettler, "Very-high-temperature stable CO₂-laser induced long-period fibre gratings," *Electron. Lett.* **35**(9), 740-742 (1999).
3. G. Rego, O. Okhotnikov, E. Dianov, and V. Sulimov, "High-temperature stability of long-period fiber gratings produced using an electric arc," *J. Lightwave Technol.* **19**(10), 1574-1579 (2001).
4. G. Humbert, and A. Malk, "Characterizations at very high temperature of electric arc-induced long-period fiber gratings," *Optics Communications* **208**(4-6), 329-335 (2002).
5. M. Iida, O. Koyama, H. Sumiana, Y. Toyooka, and M. Yamada, "High-temperature attenuation peak behaviors of long-period fiber grating inscribed with CO₂ laser," in the 19th OptoElectronics and Communications Conference (OECC), Technical Digest (2014), 484-486.
6. M. Matsui, T. Murakami, O. Koyama, S. Takasuka, A. Kusama, and M. Yamada, "High temperature characteristic of LPFG fabricated with CO₂ laser under long-term heating," in the 22th OptoElectronics and Communications Conference (OECC), Technical Digest (2017), P3-084.
7. V. R. Mamidi, S. Kamineni, L. N. S. P. Ravinuthala, S. S. Madhuvarasu, V. R. Thumu, V. R. Pachava, and K. Putha, "Fiber Bragg grating-based high temperature sensor and its low cost interrogation system with enhanced resolution," *Optica Applicata* **44**(2), 299-308 (2014).
8. Y. Tsutsumi, T. Hase, M. Ohashi, Y. Miyoshi, and H. Kubota, "Low-cost temperature sensors using mechanical long period fiber grating in 850 nm-wavelength range," in the 22th OptoElectronics and Communications Conference (OECC), Technical Digest (2017), S1593.
9. Y. Ding, X. Dai, and T. Zhang "Low-cost fiber-optic temperature measurement system for high-voltage electrical power equipment," *IEEE Transactions on Instrumentation and Measurement* **59**(4), 923-933 (2010).
10. M. Matsui, O. Koyama, A. Kusama, T. Murakami, and M. Yamada, "Temperature-sensing system employing long-period fiber grating in optical IP network," in the 23th OptoElectronics and Communications Conference (OECC), Technical Digest (2018), P2-23.
11. J. Postel, "Internet Control Message Protocol," STD 5, RFC 792, DOI 10.17487/RFC0792, (1981), <https://www.rfc-editor.org/info/rfc792>.
12. R. Presuhn, "Management Information Base (MIB) for the Simple Network Management Protocol (SNMP)," STD 62, RFC 3418, DOI 10.17487/RFC3418, (2002), <https://www.rfc-editor.org/info/rfc3418>.
13. J. Case, M. Fedor, M. Schoffstall, and J. Davin "Simple Network Management Protocol (SNMP)", RFC 1157, DOI 10.17487/RFC1157, (1990), <https://www.rfc-editor.org/info/rfc1157>.
14. O. Koyama, M. Yamada, Y. Okada, K. Matsuyama, and Y. Katsuyama, "Bidirectional amplification module for IP-over-CWDM ring network," *IEICE Trans. Commun.* **E94-C**(7), 1153-1159 (2011).
15. T. Murakami, O. Koyama, A. Kusama, M. Matsui, and M. Yamada, "Loss peak adjustment of long period fiber grating fabricated with CO₂ laser by applying tension," *IEICE Electron. Express* **15**(23), 1-7 (2018).
16. T. Erdogan, V. Mizrahi, P. J. Lemaire, and D. Monroe, "Decay of ultraviolet-induced fiber Bragg gratings," *Journal of Applied Physics* **76**(1), 73-80 (1994).